Intercomparison of a portable and two stationary mobility particle sizers for nanoscale aerosol measurements

A. S. Fonseca, M. Viana, N. Pérez, A. Alastuey, X. Querol, H. Kaminski, A. M. Todea, C. Monz & C. Asbach

View supplementary material

Published online: 20 Apr 2016.

Submit your article to this journal

Article views: 2010

View related articles

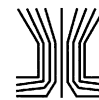View Crossmark data

Citing articles: 6 View citing articles

Taylor & Francis
Taylor & Francis Group

Intercomparison of a portable and two stationary mobility particle sizers for nanoscale aerosol measurements

A. S. Fonseca[a,b], M. Viana[a], N. Pérez[a], A. Alastuey[a], X. Querol[a], H. Kaminski[c], A. M. Todea[c], C. Monz[d], and C. Asbach[c]

[a]Institute of Environmental Assessment and Water Research (IDÆA-CSIC), Barcelona, Spain; [b]Facultad de Química, Universidad de Barcelona, Barcelona, Spain; [c]Air Quality & Sustainable Nanotechnology Unit, Institute of Energy and Environmental Technology (IUTA), Duisburg, Germany; [d]Institute for the Research on Hazardous Substances (IGF), Bochum, Germany

ABSTRACT

During occupational exposure studies, the use of conventional scanning mobility particle sizers (SMPS) provides high quality data but may convey transport and application limitations. New instruments aiming to overcome these limitations are being currently developed. The purpose of the present study was to compare the performance of the novel portable NanoScan SMPS TSI 3910 with that of two stationary SMPS instruments and one ultrafine condensation particle counter (UCPC) in a controlled atmosphere and for different particle types and concentrations.

The results show that NanoScan tends to overestimate particle number concentrations with regard to the UCPC, particularly for agglomerated particles (ZnO, spark generated soot and diesel soot particles) with relative differences >20%. The best agreements between the internal reference values and measured number concentrations were obtained when measuring compact and spherical particles (NaCl and DEHS particles). With regard to particle diameter (modal size), results from NanoScan were comparable < [± 20%] to those measured by SMPSs for most of the aerosols measured.

The findings of this study show that mobility particle sizers using unipolar and bipolar charging may be affected differently by particle size, morphologies, particle composition and concentration. While the sizing accuracy of the NanoScan SMPS was mostly within ±25%, it may miscount total particle number concentration by more than 50% (especially for agglomerated particles), thus making it unsuitable for occupational exposure assessments where high degree of accuracy is required (e.g., in tier 3). However, can be a useful instrument to obtain an estimate of the aerosol size distribution in indoor and workplace air, e.g., in tier 2.

1. Introduction

Associations between exposure to ultrafine particles (particles of low solubility with equivalent aerodynamic diameters <100 nm) and adverse health effects have been identified (Dockery et al. 1993; Atkinson et al. 2001; Kreyling et al. 2002; Oberdörster et al. 2004, 2005; Maynard and Kuempel 2005; Donaldson et al. 2006). Epidemiological studies have shown that at similar mass concentrations, ultrafine particles can be more harmful than micrometer-size particles due to their ability to penetrate deeper into the lung (Peters et al. 1997; Oberdörster et al. 2005). Taking into account that nanoscale particles typically contribute negligibly to total mass concentrations, there is evidence that other metrics such as particle number (*PN*) concentration are more sensitive for this type of particles (Kuhlbusch et al. 2011). In order to assess exposure to potentially health hazardous particles, measurements of particle diameter and mean size are also advisable.

Different instruments have been developed to quantify airborne *PN* concentrations such as condensation particle counters - CPC (Agarwal and Sem 1980; Wiedensohler et al. 1997; Hermann et al. 2007) for the determination of total *PN* concentration, and mobility particle size spectrometers such as differential mobility particle sizer (DMPS; Kousaka et al. 1985; ten Brink et al. 1983), scanning mobility particle sizer (SMPS;

Wang and Flagan 1989, 1990) or fast mobility particle sizer (FMPS; Tammet et al. 2002) for the measurement of *PN* concentrations as a function of particle size, i.e., particle number size distributions.

The theoretical principle of mobility particle size spectrometers is that particles of a specific charge distribution (Fuchs 1963) may be classified in a differential mobility analyser (DMA; Knutson and Whitby 1975; Winklmayr et al. 1991; Fissan et al. 1996; Chen et al. 1998) according to their electrical mobility. To obtain the mobility distribution, the electric field strength inside the classifier is sequentially (Fissan et al. 1983) or continuously (Wang and Flagan 1990) ramped to give the bandwidth of electrical mobilities. Typically the particles exiting the classifier are counted as *PN* with a CPC (Agarwal and Sem 1980). However, during occupational exposure studies, the use of conventional SMPS conveys transport and application limitations, due to its need for a radioactive or X-ray neutralizer and its bulky nature. Therefore, a novel portable nanoparticle sizing and counting instrument (NanoScan SMPS TSI 3910; Tritscher et al. 2013) was recently commercialized for real-time nanoparticle measurements within the range from 10 to 420 nm. This device incorporates a nonradioactive unipolar diffusion charger (corona jet type) (Medved et al. 2000), a radial differential mobility analyzer (rDMA; Zhang et al. 1995; Fissan et al. 1998) and an isopropanol-based CPC. The main advantage of this instrument is its portability (<9 kg), battery operation without the need to use power supply, small size (LxWxH = 45 × 23 × 39 cm), and the use of a nonradioactive unipolar charger which makes it a suitable monitor for real-time workplace measurements without the transport and application restrictions currently affecting traditional SMPS instruments. Another advantage is the use of isopropanol instead of butanol as a working fluid since it is a relatively benign chemical when compared to butanol (TSI 2015). The downside of the NanoScan is its lower sizing resolution (only 13 channels) (Stabile et al. 2014). Several studies have reported that based on unipolar diffusion charging of the FMPS, particles are wrongly sized in the upper working size range (Price et al. 2014; Levin et al. 2015; Zimmerman et al. 2015).

To date, few studies have measured the total *PN* concentrations and particle number size distributions by using the above mentioned methods/instruments in a variety of settings and environments such as ambient air (Wehner et al. 2002; Costabile et al. 2009; Watson et al. 2011; Reche et al. 2011; Asmi et al. 2011; Cusack et al. 2013; Beddows et al. 2014; Brines et al. 2015; Gómez-Moreno et al. 2015), indoor air (Morawska et al. 2009a; Buonanno et al. 2010; Zhang et al. 2010; Buonanno et al. 2013; Voliotis et al. 2014) and industrial and

nanotechnology-related workplaces (Demou et al. 2008; Brouwer 2010; Kuhlbusch et al. 2011; Koivisto et al. 2012; Koivisto et al. 2014; Fonseca et al. 2015a, b).

Intercomparisons between stationary mobility particle size spectrometers and CPCs can be found in the literature (Jeong and Evans 2009; Asbach et al. 2009; Watson et al. 2011; Asbach et al. 2012; Wiedensohler et al. 2012; Kaminski et al. 2013; Price et al. 2014). However, intercomparisons between stationary SMPS and the novel portable NanoScan are scarce. Only recently, Tritscher et al. (2013) studied the comparability between the NanoScan SMPS, two research-grade SMPS reference systems and an ultrafine butanol CPC. Although a good comparability was found, there is still a need to determine the reproducibility of data provided by the NanoScan and study how it relates to other sampling instruments in order to scrutinize the limits concerning different materials, concentrations, particle shapes and sizes. Stabile et al. (2014) compared the NanoScan and an SMPS with a variety of different polydisperse test aerosols. They found that the agreement was best for spherical particles, whereas significant deviations were observed for agglomerates. They furthermore found a better agreement between the NanoScan and the SMPS when no diffusion and multiple charge corrections were applied to the latter. It should, however, be noted that only data from an SMPS with both corrections active can be considered as the most accurate representation of a particle size distribution, whereas SMPS data obtained without these corrections are known to be flawed, especially in the case of the larger, e.g., DEHS particles, where the fraction of multiply charged particles is significantly higher and needs to be corrected using the multiple charge correction (Kaminski et al. 2013). Reineking and Porstendörfer (1986) reported that diffusional losses of particles inside a TSI long DMA are equivalent to losses in a 13 m long tube. As an example, losses of 20 nm particles in a long DMA amount to approximately 66% and of 10 nm particles to approximately 75%. Diffusional losses of particularly small particles can, therefore, be quite significant and need to be corrected for. Deconvolution of the NanoScan raw data is much more complex than for the SMPS data and, therefore, the multiple charge and diffusion loss correction are already inherently included in the empirical data evaluation routines. In the present study, only SMPS data that had been corrected for multiple charge effects and diffusion losses were used.

The purpose of the present study was to compare the performance of the portable NanoScan SMPS TSI 3910 with that of two stationary SMPS instruments (with a long and a nano DMA) and one ultrafine butanol

condensation particle counter (UCPC) in a controlled atmosphere and for different particle types. The ultimate goal was to assess the suitability of the NanoScan instrument for occupational exposure studies, given their specific needs with regard to accuracy, transport and use limitations, etc. The instruments were simultaneously challenged with intentionally produced particles covering a wide range of particle sizes and morphologies: diethyl-hexyl-sebacate (DEHS; spherical), sodium chloride (NaCl; cubic or near spherical shape), and agglomerates as zinc oxide (ZnO), spark generated soot and diesel soot particles (Kaminski et al. 2013).

2. Methodology

2.1. Instrumentation

Two common stationary and one NanoScan SMPS were used for measuring particle size distributions. In addition, for measuring total size-integrated number concentrations, an ultrafine CPC was used (Table 1).

The two stationary SMPS used as internal reference for the size distribution in this study were: (i) SMPS (TSI, Model 3936 long), which consists of a long-column DMA (TSI, Model 3081; Liu and Pui, 1974) and a butanol CPC (TSI, Model 3772) with a lower detection limit of 10 nm, hereafter referred to as "SMPS-L" and (ii) SMPS (TSI, Model 3936 nano), which consists of a nano-DMA (TSI, Model 3085; Chen et al. 1998) and an Ultrafine Water-based Condensation Particle Counter with a lower detection limit of 2.5 nm (UWCPC, TSI, Model 3786; Hering et al. 2005), hereafter referred to as "SMPS-N." Both SMPS used a ^{85}Kr bipolar neutralizer with an initial activity of 74 MBq (TSI, Model 3077). The neutralizer used in SMPS-N was approximately 5 years old and the one in SMPS-L more than 10 years. In the

measuring configurations selected for this study, both SMPS-L and SMPS-N delivered size distributions available in 64 channels per size decade. SMPS-L measured in the size range 9.7 nm $\leq D_p \leq$ 421.7 nm (0.6 L min^{-1} aerosol, 6 L min^{-1} sheath flow rate) or 19.1 nm $\leq D_p \leq$ 897.7 nm (0.2 L min^{-1} aerosol, 2 L min^{-1} sheath flow rate) whereas the SMPS-N in the size range 3.2 nm $\leq D_p \leq$ 107.5 nm (0.6 L min^{-1} aerosol, 6 L min^{-1} sheath flow rate). The aerosol flow rate was frequently checked by using a flow meter (TSI, Model 4045) to ensure it remained ±10% of the instrumental flow rate. The SMPS with long DMA was equipped with an impactor (nozzle diameter 0.0508 cm) which removes all particles >553 nm (aerodynamic diameter) at an aerosol flow rate of 0.6 L min^{-1} and >1011 nm at a flow rate of 0.2 L min^{-1}. The SMPS with nanoDMA was equipped with an impactor with a 0.071 cm nozzle with a cut off size around 1 μm. The latter impactor was mainly used to protect the instrument from larger particles, because no impactor with a cut-off size matching the upper size limit of the DMA is available. Data were collected and evaluated with the TSI Aerosol Instrument Manager software (AIM, version 9.0.0.0, TSI), which allows correcting for particle diffusion losses inside the instruments based on empirical factors as well as for multiple charge correction (Hoppel 1978; Fissan et al. 1983). The time resolution of both SMPSs was set to 180 sec (120 s upscan, 30 s retrace and 30 s wait time for SMPS-L and 120 s upscan, 20 s retrace and 40 s wait time for SMPS-N, respectively).

While SMPSs are generally used to measure stable particle size distributions, the time resolution of the portable electrical mobility spectrometer NanoScan SMPS (TSI, Model 3910; aerosol flow rate 0.75 L min^{-1} ± 20% flow inlet) allows in principle for measuring more rapidly changing particle mobility size distributions in 13 channels. In this study, while the stationary SMPS delivered

Table 1. Specifications of instruments used in this study.

ID	Manufacturer and Model	Studied metric	Size range [nm]	Time resolution [s]	Aerosol flow rate [L min^{-1}]	Sheath flow rate [L min^{-1}]	Software version	Other settings
SMPS-L	TSI SMPS, Model 3936 long	PNC[a] + PSD[b]	9.7–421.7 19.1–897.7	180	0.6 0.2	6 2	AIM, version 9.0.0.0	Long DMA (TSI, Model 3081) + CPC (TSI, Model 3772) ^{85}Kr bipolar neutralizer (74 MBq, TSI model 3077)
SMPS-N	TSI SMPS, Model 3936 nano	PNC[a] + PSD[b]	3.2–107.5	180	0.6	6	AIM, version 9.0.0.0	Nano DMA (TSI, Model 3085) + UWCPC (TSI, Model 3786) ^{85}Kr bipolar neutralizer (74 MBq, TSI model 3077)
NanoScan	TSI SMPS, Model 3910	PNC[a] + PSD[b]	10–420	60	0.75	–	NanoScan Manager Version 1.0.0.19	Non-radioactive unipolar diffusion charger (corona jet type)
UCPC	TSI UCPC, Model 3776	PNC[a]	2.5–3000	1	1.5	–	AIM, version 9.0.0.0	–

[a]PNC: *PN* concentration; [b]PSD: particle size distribution.

size distribution data every 3 min, the time resolution of the NanoScan SMPS was 1 min (45 s up-scan in which the measurement occurs, and a 15 s retrace).

An ultrafine butanol condensation particle counter (UCPC, TSI, Model 3776) was used as internal reference to determine the total number concentration. According to the manufacturer's specifications, the UCPC covers the size range between 2.5 nm and 3 μm and uses a single particle count mode measuring up to 3×10^5 cm^{-3}. The UCPC was operated in high flow mode with a flow rate of 1.5 L min^{-1} in order to minimize particle diffusion losses in the system. Particle losses were not corrected, because the UCPC does not record size distributions, which are required for correction of diffusional losses.

In order to confirm the particle morphology and the elemental chemistry of spark generated soot and diesel particles, samples were collected onto Quantifoil® gold (Au) grids with 1 μm diameter holes - 4 μm separation of 200-mesh with the nanometer aerosol sampler (NAS; TSI, Model 3089; Dixkens and Fissan 1999) for transmission electron microscopy (TEM) and energy dispersive x-ray spectroscopy (EDS) analysis. Charged particles in the range from 2 to 100 nm were sampled onto collection substrates for 10 min at a flow rate of 2.5 L min^{-1} and a collection voltage of +10 kV.

2.2. Particle generation

Four different types of aerosol generators were used to intentionally produce five different types of aerosol: (i) NaCl; (ii) DEHS; (iii) ZnO; (iv) spark generated soot, and (v) diesel soot. A total of fifteen experiments were performed, to assess the performance of the instruments under different concentration levels and different particle sizes. Twelve of these experiments corresponded to aerosols with unimodal particle size distribution and the remaining three were multimodal (Table S1 in the online supplementary information [SI]).

Cubic (NaCl) particles with average sizes of 10 nm and 60 nm were produced by a burner (FG2, MoTec Konzepte, Bochum Germany; Monsé et al. 2014) and a home-made atomizer, respectively. ZnO particles with average particle size of 60 nm were generated by using the same burner generator, while small droplets of DEHS were generated by spraying pure DEHS using the aforementioned atomizer.

Agglomerated carbonaceous aerosol (spark generated soot) were produced using a spark generator (GFG 3000, Palas GmbH, Karlsruhe, Germany) equipped with graphite electrodes. The total spark generator current was always 14.6 mA and the argon flow rate approximately 5 L min^{-1}. The generator allows for a dilution of the freshly produced aerosol with particle-free dilution air to avoid rapid coagulation. A dilution air of 17.5 L min^{-1} during experimental runs for the smallest spark generated soot in diameter (#8 and #9), and 5 L min^{-1} during experimental runs for the largest spark generated soot in diameter (#10 and #11), were added. The highly concentrated aerosol was further diluted in a wind tunnel with filtered air ranging from 200 to 2880 m^3 h^{-1}. The use of different dilution rates, allowed to understand the performance of the instruments under two different concentration levels, around 10^4 cm^{-3} and 10^5 cm^{-3}. An average particle size of 48 and 67 nm was obtained for experiments spark generated soot #8 and #9, respectively, whereas for spark generated soot #10 and #11, particles of 82 and 105 nm in diameter were obtained.

Agglomerated diesel soot particles ($\sim$100 nm), were generated by using a diesel engine (aspiration type, 2180 cm^3, Mercedes Benz 220D, 44 kW at 4200 rotations min^{-1}) idling at 1400 rotations min^{-1}.

Additionally, bimodal size distributions were produced from diesel soot by letting the same diesel engine idling at 800 rotations min^{-1} and NaCl by using burner and NaCl/DEHS trimodal size distributions by a combination of burner and atomizer. For the ZnO, diesel soot and multimodal particle size distributions, only one concentration level was chosen.

All the measured concentrations were within the range specified by the manufacturers for the instruments included in the study.

2.3. Experimental setup

Experiments were conducted at the NanoTest-Center of the Institute for the Research on Hazardous Substances (IGF) in Dortmund, Germany. Details of the Nano Test Center can be found in Asbach et al. (2009, 2012) and Kaminski et al. (2013).

Particles from the atomizer and spark generator were neutralized before being introduced into the wind tunnel by passing through a radioactive source ^{85}Kr (TSI, Model 3012A; 370 MBq initial activity, approximately 3 years old). Particles from the atomizer were additionally dried by a silica gel diffusion dryer. Afterwards, they were injected into the wind tunnel (20 m long with a diameter of 0.7 m), where they were mixed with ultra-low penetration air (ULPA) filtered dilution air. The wind tunnel feeds into a 20 m^3 exposure chamber, which is ventilated by a blower that defines the dilution air flow rate in the wind tunnel. A schematic diagram of experimental setup is shown in Figure S1 in the SI.

The dilution air flow rates in the wind tunnel were adjusted to flow rates between 250 and 3660 m^{3h-1} in

order to produce the desired particle concentration levels. According to Asbach et al. (2012), the aerosol is homogenously mixed in the exposure chamber so that all instruments placed inside sample identical aerosol concentrations and particle size distributions.

All devices were placed in the mixing chamber and sampled directly without any tubes attached. They were positioned on a table inside the exposure chamber (Figure S1 in the SI), measuring at approximately the same height with adequate distance between each other. The NAS, which required frequent replacement of TEM grids, was placed outside the exposure chamber and connected to a sampling train, operated at 20 L min^{-1}, which splits the total flow into two flows of 10 L min^{-1}.

Before each experimental run, the mixing chamber was flushed with clean air until the background concentration in the exposure chamber reached a level of typically around 1×10^3 cm^{-3} or below, and after that the respective aerosol generator was connected to the wind tunnel. Measurements started approximately 20 min after the generator was switched on, when the N concentration in the chamber was constant ($\pm 10\%$). Each experiment consisted of 30 consecutive minutes of particle measurements under stable PN concentrations.

2.4. Data analysis

Regarding the measured size distribution data, since the SMPSs and NanoScan instruments use different size channel widths and midpoints, data fitting of the measured size distributions was necessary. Thus, for a quantitative comparison of the measurement results, each experiment data was averaged for the approximately 30 min period and afterwards fitted to lognormal particle number size distributions (characterized by parameters as total number concentration, mode diameter, and standard deviations). Fitting was conducted using the multi-peak fit option of IGOR version 6.2.0.0. The

distributions were fitted within the size limits of SMPSs. The probability value (*p-value*) calculated by the Two Sample t Test (unequal variances) provided insights into the quality of the fitting procedure. If the *p-value* is less than or equal to the significance level (α, most often set at *p-value* ≤ 0.05), the test suggests that the observed data are inconsistent with the null hypothesis (that the means of two datasets are equal), so the null hypothesis must be rejected. This test guarantees that the type I error rate (is the incorrect rejection of a true null hypothesis) is at most α. In this study, a *p-value* ≥ 0.05 was considered acceptable in data fitting.

3. Results and discussion

3.1. Unimodal aerosols

The comparison between the response of the NanoScan SMPS with the internal reference response for size distribution (SMPS-L and SMPS-N) and total *PN* concentrations (UCPC) to unimodal aerosols is shown in Table 2 and Table 3 for compact spherical and agglomerated particles, respectively. It should be noted that the size range of both SMPS-N and SMPS-L is limited due to the nano-DMA and long-DMA, respectively, and therefore only in case of the aerosol size range in experiment #1 NaCl was properly covered by SMPS-N and in case of experiments #4, #5 and #6 DEHS, were only covered by SMPS-L. In the case of spark generated soot #10 #11 and diesel soot #12, only the SMPS-L data was used for intercomparison since the SMPS-N size distribution was incomplete and the multiple charge correction was not usable, because it requires the use of an impactor that removes all particles larger than the largest particle size covered by the DMA with the settings used. Such an impactor is not available.

As shown in Tables 2 and 3, the variability across instruments was broad for each specific type of aerosol, even at times between the two SMPS instruments. These

Table 2. Parameters of the fitted lognormal particle number size distributions (total number concentrations, modal diameter, and standard deviations) measured by the SMPSs (NanoScan, SMPS-L, and SMPS-N) and UCPC measuring compact and spherical particles (number 1–6 in Table S1 in the SI); all concentrations (PN_{total}) in [cm^{-3}] and all diameters (D_{mode}) in [nm].

		NaCl			DEHS		
Experiment		#1	#2	#3	#4	#5	#6
UCPC $PN_{total} \pm \sigma$ [cm^{-3}]		**$7.9 \pm 0.3 \times 10^4$**	**$1.8 \pm 0.3 \times 10^4$**	**$1.6 \pm 0.7 \times 10^5$**	**$2.1 \pm 0.03 \times 10^4$**	**$9.9 \pm 0.2 \times 10^4$**	**$4.2 \pm 0.3 \times 10^4$**
NanoScan	$PN_{total} \pm \sigma$ [cm^{-3}]	$2.1 \pm 0.1 \times 10^4$	$1.8 \pm 0.4 \times 10^4$	$2.1 \pm 0.2 \times 10^5$	$2.3 \pm 0.02 \times 10^4$	$1.0 \pm 0.1 \times 10^5$	$5.1 \pm 0.6 \times 10^4$
SMPS-L		*	$1.6 \pm 0.3 \times 10^4$	$1.7 \pm 0.1 \times 10^5$	$2.1 \pm 0.04 \times 10^4$	$1.0 \pm 0.05 \times 10^5$	$4.0 \pm 0.3 \times 10^4$
SMPS-N		$7.8 \pm 0.5 \times 10^4$	$1.7 \pm 0.3 \times 10^4$	$1.9 \pm 0.1 \times 10^5$	*	*	*
NanoScan	$D_{mode} \pm \sigma$ [nm]	13.2 ± 0.09	72.9 ± 2.4	68.6 ± 2.1	173.6 ± 2.5	182.2 ± 2.6	131.6 ± 1.6
SMPS-L		*	**64.3 ± 0.3**	**58.7 ± 0.3**	**231.2 ± 3.9**	**228.2 ± 1.4**	**198.8 ± 1.3**
SMPS-N		**10.6 ± 0.04**	73.6 ± 1.3	64.3 ± 0.6	*	*	*

σ: Standard deviation.
*Non-overlapping size.
Values in bold: considered internal reference value for total N concentration (UCPC) and for particle number size distributions (SMPS-N or SMPS-L).

Table 3. Parameters of the fitted lognormal particle number size distributions (total number concentrations, modal diameter, and standard deviations) measured by the SMPSs (NanoScan, SMPS-L and SMPS-N) and UCPC measuring agglomerated particles (number 7 to 12 in Table S1 in the SI); all concentrations (PN_{total}) in [cm^{-3}] and all diameters (D_{mode}) in [nm]. Values in bold: considered internal reference value for total PN concentration (UCPC) and for particle number size distributions (SMPS-N or SMPS-L).

| | | ZnO | Spark Generated Soot | | | | Diesel Soot |
Experiment		#7	#8	#9	#10	#11	#12
UCPC $PN_{total} \pm \sigma$ [cm^{-3}]		**1.3 ± 0.03 × 10^5**	**1.5 ± 0.02 × 10^4**	**1.0 ± 0.02 × 10^5**	**1.1 ± 0.02 × 10^4**	**7.9 ± 0.2 × 10^4**	**1.2 ± 0.09 × 10^5**
NanoScan	$PN_{total} \pm \sigma$ [cm^{-3}]	1.8 ± 0.2 × 10^5	1.8 ± 0.1 × 10^4	1.4 ± 0.1 × 10^5	1.6 ± 0.02 × 10^4	1.3 ± 0.05 × 10^5	1.9 ± 0.2 × 10^5
SMPS-L		1.5 ± 0.09 × 10^5	1.6 ± 0.1 × 10^4	1.1 ± 0.04 × 10^5	1.1 ± 0.02 × 10^4	7.2 ± 0.3 × 10^4	1.2 ± 0.1 × 10^5
SMPS-N		1.5 ± 0.1 × 10^5	1.8 ± 0.2 × 10^4	1.1 ± 0.03 × 10^5	*	*	*
NanoScan	$D_{mode} \pm \sigma$ [nm]	67.4 ± 0.9	49.1 ± 0.7	63.2 ± 0.9	74.6 ± 1.1	91.1 ± 1.7	95.1 ± 1.5
SMPS-L		**66.2 ± 0.3**	**47.9 ± 0.3**	**66.7 ± 0.2**	**81.9 ± 0.2**	**105.4 ± 0.2**	**95.6 ± 0.5**
SMPS-N		66.9 ± 0.3	48.6 ± 0.3	70.7 ± 0.5	*	*	*

σ: Standard deviation.
*Non-overlapping size.

data should be interpreted bearing in mind the different size ranges measured by each of the instruments, which may significantly influence the total *PN* concentrations measured. To support the interpretation of these Tables, Figure 1 shows the differences in total *PN* concentration between the three instruments and the UCPC while Figure 2 shows the relative differences in modal diameters between NanoScan and the other SMPSs.

Overall, for aerosols >50 nm NanoScan measured higher *PN* concentrations than the internal reference UCPC, with deviations between 4% and 66% (Figure 1 and Tables 2 and 3). The largest deviations of the total *PN* from the reference instrument UCPC were observed for agglomerated particles although, these type of particles registered the lowest standard deviations (<±11%; error bars shown in Figure 1).
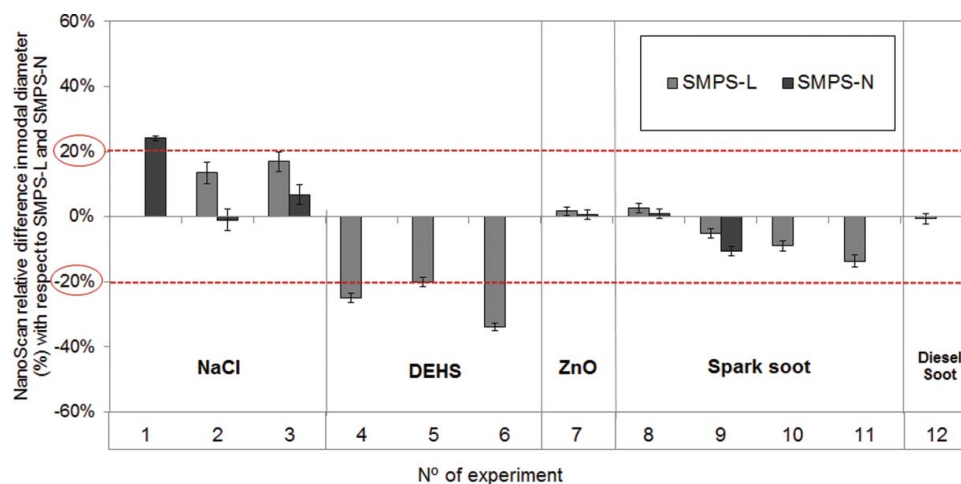
If an arbitrary threshold of 20% difference (representing a worthy performance for a field instrument, and also the sum of the +/−10% uncertainty of CPC instruments) between *PN* measured (NanoScan, SMPSs) and *PN* expected (UCPC) is considered, the results obtained with NanoScan were above threshold for 7 of the aerosols (NaCl #1 and #3; ZnO #7; spark generated soot #9, #10 and #11; and diesel soot #12) whereas a good agreement (below threshold) was obtained for 2 of the aerosols for which SMPS-N covered most of the particle size distribution (NaCl #1 and ZnO #7) and for all unimodal aerosols with SMPS-L, excepting NaCl #1 (which is not covered by SMPS-L).

Contrary to the total *PN* concentrations, the particle modal diameter measured by NanoScan and SMPS-L (Figure 2) agreed poorly (>20% difference) for DEHS particles, but agreed fairly well within <10% deviation for 66 nm ZnO, 48 and 67 nm spark generated soot at low and high concentrations, 82 nm spark generated soot at low concentrations and 96 nm diesel soot.
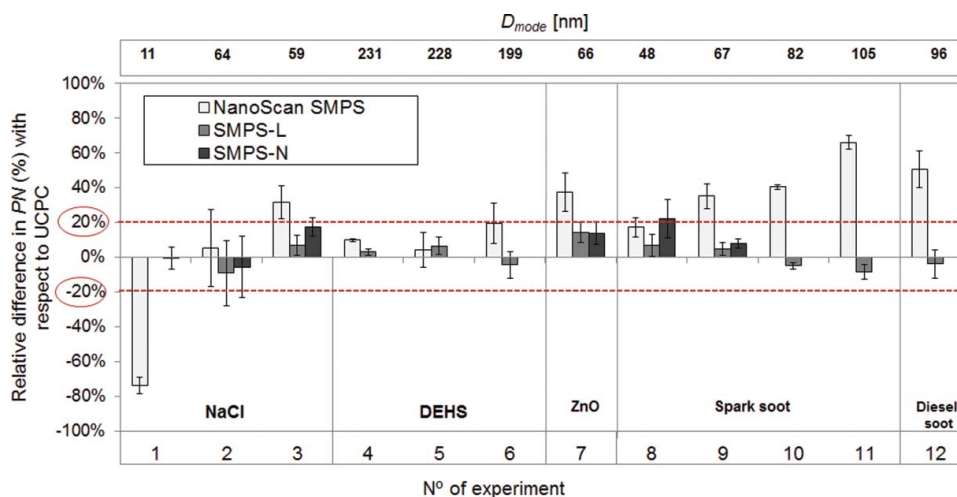
Figure 1. Relative difference in *PN* concentration between the three SMPSs and UCPC measurement. Error bars indicate the standard deviation (±σ). The dashed (red) horizontal line indicates the considered arbitrary threshold of ±20% difference between *PN* measured (NanoScan, SMPSs) and *PN* expected (UCPC).

Figure 2. Relative difference in modal diameter between NanoScan and SMPS-L measurement (gray columns) and SMPS-N (black column). Error bars indicate the standard deviation ($\pm\sigma$). The dashed (red) horizontal line indicates the considered arbitrary threshold of $\pm20\%$ difference between PN measured (NanoScan, SMPSs) and PN expected (UCPC).

Detailed information concerning the performance of each instrument as the measured total PN concentration and particle size distribution for each type of aerosol under study is shown and discussed in the following sections.

3.1.1. Compact and spherical particles

In the NaCl experiments, it is important to take into account that the generated aerosol was outside the measurement range of the SMPS-L (19.1–897.7 nm) and in lower end of the NanoScan particle size measurement range for 11 nm NaCl #1 and that SMPS-N did not cover the entire range of the generated 60 nm NaCl #2 and #3. When comparing total PN between the different instruments and the UCPC (considered here as the internal reference instrument), results showed that, for 11 nm NaCl #1 particles, PN concentrations were significantly underestimated (p-value < 0.05) by the NanoScan (74 $\pm$ 5%). Total PN concentration reported by the SMPS-N agreed with the reference (1% underestimation; p-value $= 0.2$). Since the generated 60 nm NaCl #2 and #3 was within the size range of the NanoScan and SMPS-L, the performance of the two instruments in terms of PN concentrations improved largely with coarser particles (when compared to 11 nm NaCl #1 particles). At low concentrations (NaCl #2), PN concentrations measured by NanoScan and SMPS-L overestimated by 5.1 $\pm$ 22% and underestimated by 9.3 $\pm$ 19%, respectively, those measured by the UCPC. At high concentrations (#3), PN was overestimated by 32 $\pm$ 10% by NanoScan and by 7 $\pm$ 6% by SMPS-L. Thus, the deviation from the reference value of NanoScan was larger at high concentrations. The size distributions measured for 11 nm NaCl #1 and 60 nm NaCl #3 are illustrated in Figures 3a and b, respectively. As for 11 nm NaCl #1, the performance of

NanoScan was far from optimal for this type of aerosol since particle size distributions deviated >20% from SMPS-N (Figures 2 and 3a). As a result, care should be
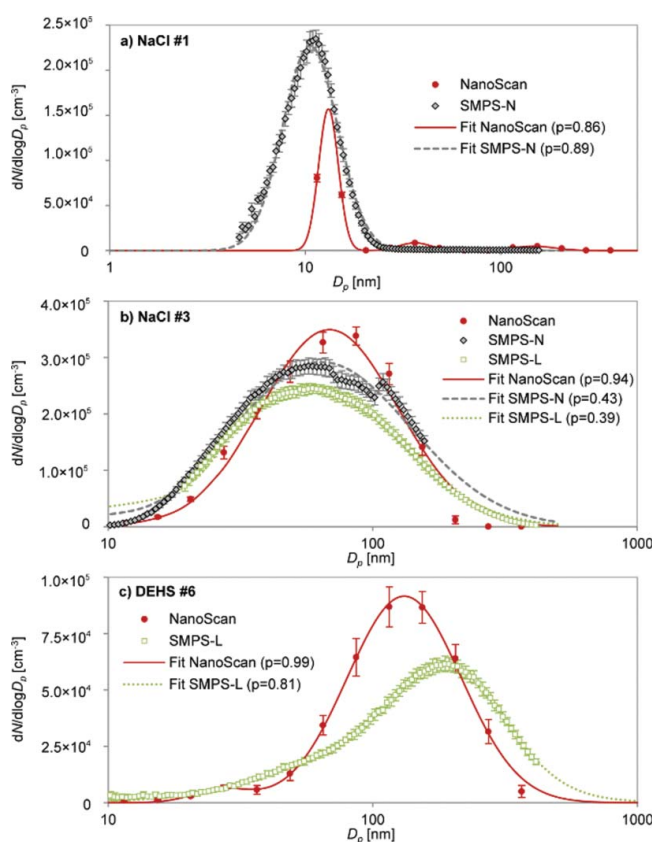
Figure 3. Measurement data and fitted particle number size distribution of generated particles measured in the exposure chamber with SMPS-N, SMPS-L and NanoScan: (a) 11 nm NaCl #1; (b) 60 nm NaCl #3 at high concentration and; (c) 199 nm DEHS #6. Error bars indicate the standard deviation. $p = p$-value.

taken when using NanoScan data from the lower end of the instrument's particle size range.

Particle size distributions of 60 nm NaCl #2 at low (Figure S2 in the SI) and NaCl #3 at high concentrations (Figure 3b) measured by NanoScan were slightly shifted towards larger particle sizes (73 and 69 nm, respectively) whereas the mode diameters measured by SMPS-L at low and at high NaCl concentrations were 64 and 59 nm, respectively. The standard deviations of mode diameters showed variations in a similarly narrow range between 0.3 and 2.4 (NaCl #2) and between 0.3 and 2.1 nm (NaCl #3). The dilution in the wind tunnel not only affected the concentrations but also influenced particle size (i.e., with an increase of the flow rate inside the wind tunnel, an increase of particle concentration and a decrease in particle diameter are detected due to the shorter residence time for coagulation). The performance of the NanoScan instrument regarding particle diameters was slightly better for low *PN* concentrations and larger NaCl particles ($1.8 \pm 0.3 \times 10^4$ cm^{-3}; 73 nm; NaCl #2; Figure 2) which was in agreement with the lowest deviations in total *PN* concentrations observed from NanoScan when compared to the reference value of UCPC. Since the particle mode shifting was more pronounced at higher concentrations of NaCl and lower diameter (69 nm; NaCl #3), the NanoScan overestimation in measuring particle number concentration may possibly be explained by a particle size misclassification in the radial DMA and a corresponding effect on the data deconvolution. However, it should be taken into account that these misclassification of particle size is within the uncertainty of 20% of deviations. In addition, this behavior was not observed for all other spherical aerosol types (e.g., DEHS, see below). Thus, further studies are needed to understand this behavior.

Spherical DEHS particles #4, #5, and #6 were mostly outside the measurement range of the SMPS-N (3.2–107.5 nm). When comparing the measured *PN* between the SMPS-L, NanoScan, and UCPC in experiments, ∼230 nm DEHS #4 and #5, results showed that *PN* was overestimated by NanoScan (10 ± 1% at low and 4 ± 10% at high concentrations) and by the SMPS-L (3 ± 2% at low and 6 ± 5% at high concentrations). Regarding the 199 nm DEHS #6 (Table 2), NanoScan measurements agreed with the reference *PN* concentration within the arbitrary 20% threshold defined above (19 ± 12% difference), while the SMPS-L underestimated the reference value with 5 ± 8% (Table 2 and Figure 1). Especially in the case of NanoScan these values should be considered with care, as the instrument did not cover the entire size range of the test aerosol. A higher overestimation of the reference values might be expected if we consider the results obtained when measuring the 199 nm DEHS #6.

However, for both NanoScan and SMPS-L an agreement within 20% is to be expected, which was the case.

For DEHS particles, the particle size distributions measured by NanoScan showed a poor agreement when compared with the ones measured by the SMPS-L (Table 1 and Figure 2). The NanoScan particle size distributions measured for ∼230 nm DEHS #4 and #5 (Figure S3 in the SI) and 199 nm DEHS #6 (Figure 3c) were shifted towards smaller particles sizes, measuring mode particle diameters of 174–182 nm and 132 nm (20–25% and 34% lower than reference value of SMPS-L, respectively). The deviations among both instruments were considered not statistically significant (*p-value* > 0.05) (Table 2 and Figure 2). This difference in NanoScan performance for the DEHS aerosols may be caused by the fact that the Cunningham slip correction factor gets an increasingly weak function of particle diameter with increasing particle size and eventually even passes a minimum (Levin et al. 2015), and hence the electrical mobility of unipolar diffusion charged particles (as acquired in the NanoScan) also becomes less sensitive in measuring the particle diameter (Morawska et al. 2009b) by acquiring a charge level which is nearly proportional to the particle diameter (Jung and Kittelson 2005; Asbach et al. 2011). It should be noted that a constant and unexpected peak was detected around 22–27 nm with NanoScan in each experimental run with DEHS particles, and it is also suggested by the SMPS-L data. Although these peaks were well below the main peak of the measured size distribution, there is no apparent reason for this occurrence and seems due to a systematic failure, e.g., due to an overcompensation in the data deconvolution.

The results from the experiments with compact and spherical particles (DEHS and NaCl aerosols) suggest that the agreement between NanoScan and SMPS concerning sizing and *PN* concentrations is dependent on the combination of total *PN* concentration and particle size, given that the better performances for NanoScan were observed while measuring aerosol NaCl concentrations in the range of 10^4 cm^{-3} (NaCl #2), and excluding those for which particle diameter was at the lower end of the measurement range of the instrument (NaCl #1).

Additionally, the lower accuracy of NanoScan (lower number of channels) and consequently, the particle size misclassification seems to be the reason for the Nanoscan overestimation in measuring particle number concentration. The higher the deviation on the mode particle size, the higher the deviations on the particle counting. From this assessment, the NanoScan underestimated particles larger than 200 nm by up to 34%, thus making it unsuitable for occupational exposure assessments where a high degree of accuracy is required. This
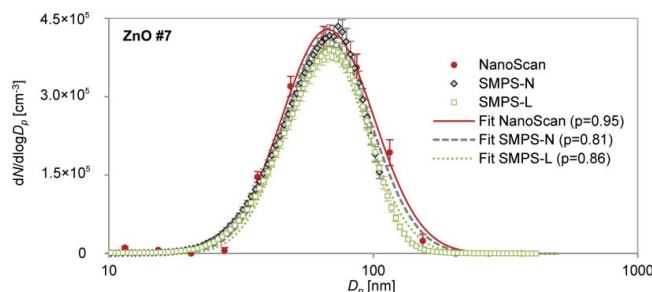
Figure 4. Measurement data and fitted particle number size distribution of generated 66 nm ZnO particles (#7), measured in the exposure chamber with SMPSs and NanoScan. Error bars indicate the standard deviation. $p = p$-value.

instrument may be advisable for tier 2 studies, with an indicative purpose and which require a lower measurement accuracy, but its use should not be encouraged for tier 3 studies.

In addition, it is important to highlight that these results cannot be generalized for all spherical particles. The recent study of Stabile et al. (2014) concluded that the spherical atomized dioctyl phthalate (DOP) particles (111 nm by SMPS with diffusion and multiple charge correction) were both correctly counted and sized. Similar results were also published by Tritscher et al. (2013), with both polydisperse NaCl and Emery Oil (EO) particles. These discrepancies highlight the need for further research in this field.

3.1.2. Agglomerated particles

While the size distribution agreement between SMPS-L and NanoScan was poor for NaCl particles with sizes around 59–64 nm and DEHS with sizes around 199–231 nm, it agreed well for the tested agglomerated 66 nm ZnO #7 (Figure 4). The size distribution measured by NanoScan showed a narrow range of modal diameter of 67.4 ± 0.9 nm. However, the total PN concentrations measured by NanoScan, SMPS-L, and SMPS-N, were $1.8 \pm 0.2 \times 10^5$, $1.5 \pm 0.1 \times 10^5$ and $1.5 \pm 0.1 \times 10^5$ cm^{-3}, with deviations from the internal reference UCPC concentration below 20% threshold for both SMPS-L and

SMPS-N, and over (37%) for NanoScan (Table 3 and Figure 1). As described above, this significant overestimation (p-value < 0.05) of the PN by NanoScan could be related to the ZnO concentrations generated (in the order of 10^5 cm^{-3}), higher than in previous NaCl experiments (in the order of 10^4 cm^{-3}) or, in this case, eventually due to the effect of particle morphology on NanoScan particle unipolar diffusion charger. Previous studies with unipolar diffusion chargers have recognized that the charging efficiency for agglomerates is different from the ones for spheres (Biskos et al. 2004; Asbach et al., 2009, 2012; Leskinen et al. 2012; Kaminski et al. 2013; Stabile et al. 2014; Zimmerman et al. 2014, 2015). Particle borne preexisting charges may also affect the charging efficiency (Qi et al. 2009; Kaminski et al. 2013).

Similarly to ZnO, the spark generated soot particle morphology deviated most from the commonly assumed spherical particle shape. The 48–67 nm spark generated soot particles were produced at low ($1.5 \pm 0.02 \times 10^4$ cm^{-3}; spark generated soot #8) and high ($1.0 \pm 0.02 \times 10^5$ cm^{-3}; spark generated soot #9) concentrations. In these experiments, SMPS-N did not cover the entire range of the generated aerosol.

When comparing total PN between the SMPSs and the internal reference UCPC, results evidenced that PN concentrations were overestimated by NanoScan above the 20% threshold ($35 \pm 7\%$ at high concentrations; spark generated soot #9) and below the threshold at low concentrations ($17 \pm 6\%$; spark generated soot #8), as well as by SMPS-L at low and high concentrations ($7 \pm 6\%$ for low concentration and $5 \pm 4\%$ for the high concentration). All these deviations were considered to be statistically significant (p-value < 0.05). The performance of SMPS-L regarding the particle count was better at higher than at lower concentrations, as opposed to NanoScan (in agreement with the results obtained in the previous experiments such as NaCl).

Corresponding TEM images for these generated spark soot particles are shown in Figure 5a whereas the particle size distributions are shown in Figure S6 in the SI. As can be confirmed, the TEM images show a presence of
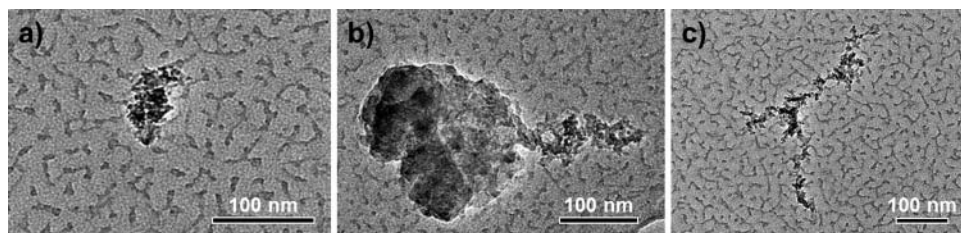
Figure 5. TEM images of collected samples: (a) 67 nm spark soot at high concentration (spark generated soot #9); (b) and (c) 105 nm spark generated soot at high concentration (spark generated soot #11).

compacted spark generated soot particles of diameter >50 nm which agrees fairly well with the delivered diameters by the instruments at high concentrations (63.2 nm spark generated soot #9 by NanoScan and 66.7 nm spark generated soot #9 by SMPS-L).

Contrary to the total *PN* concentrations measured by NanoScan, the instruments performances regarding particle size distributions were almost identical at high and low concentrations with $3 \pm 1\%$ and $5 \pm 1\%$ difference from the reference, respectively (Figure 2 and Figure S4 in the SI).

Since the NanoScan agreement regarding particle size was better for agglomerated particles (48–67 nm spark generated soot #8 and #9 and 66 nm ZnO #7) than for compact particles (59–64 nm NaCl #2 and #3), it can be concluded that the performance of this instrument not only depends on effective particle size but also on particle morphology. Different charging probabilities of the bipolar (SMPSs) and unipolar diffusion charger (NanoScan) under differently shaped particles may be a hypothesis for this dependence. It has been reported that charging is affected by particle morphology (Asbach et al. 2009; Kaminski et al. 2013; Zimmerman et al., 2014, 2015).

Subsequently, the instruments were exposed to larger spark generated soot particles of 82 nm and 105 nm in diameter using the same settings: low ($1.1 \pm 0.02 \times 10^4$ cm^{-3}; spark generated soot #10) and high ($7.9 \pm 0.2 \times 10^4$ cm^{-3}; spark generated soot #11) concentrations.
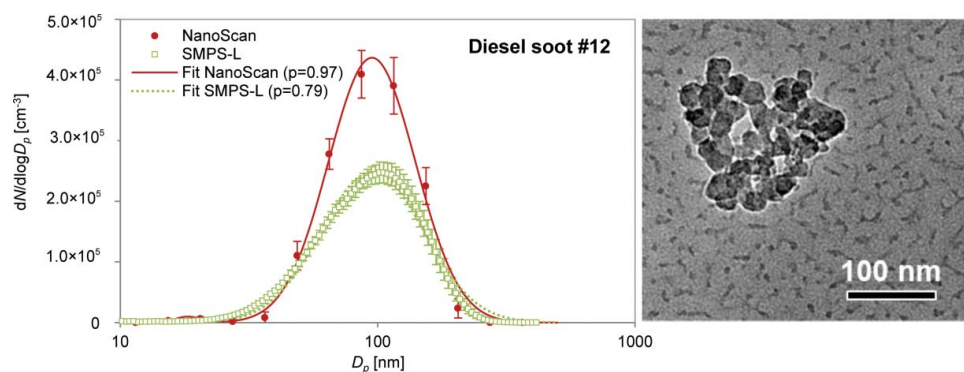
The *PN* concentrations measured by NanoScan significantly overestimated, $40 \pm 1\%$ and $66 \pm 4\%$, those measured by the internal reference UCPC at low and high concentrations, respectively (spark generated soot #10 and #11). As in the case of *PN* concentration with 48–67 nm spark generated soot #8 and #9, the performance of NanoScan decreased from lower to higher concentrations, despite both scenarios being in the order of 10^4 cm^{-3} (Figure 1). Concerning SMPS-L, different behaviors were observed in comparison to those registered for 48–67 nm spark soot, since the *PN* concentrations were underestimated for low (by $5 \pm 2\%$) (spark generated soot #10) and for high concentrations (by $9 \pm 4\%$) (spark generated soot #11).

The corresponding size distributions are shown in Figure S5. Spark generated soot particles sampled on TEM grids are shown in Figures 5b and c. The TEM images show that the spark soot particle sizes were larger than those reported by all of the instruments, evidencing that all of them underrepresented the actual spark generated soot particle size (>100 nm) delivering an electrical mobility diameter much smaller than the geometric extension of the agglomerate spark soot (seen in Figure 5c) and unstructured appearance (seen in Figure 5b). The Figure 5c suggests that the particles were aligned in the electric field and thus, classified as mobility diameter smaller than the particle length itself. However, from Figure 5b it seems that there is two overlapping particles, a less structured and larger particle on the left side (>200 nm) and a more structured particle on the right side of approximately 100 nm as diameter which agrees well with the instrument's response.

As can be seen, the resulting spark generated soot size distributions measured by NanoScan showed smaller modal diameters (75–91 nm; Table 3) than the internal reference SMPS-L (82–105 nm). In agreement with previous experiments, as in the case of total *PN* concentrations, the shift towards smaller particle sizes according NanoScan was more evident at high particle concentrations. Also, by comparing both spark generated soot particles (48–67 nm and 82–105 nm), the reported effects were more pronounced by NanoScan when the spark soot agglomerates were larger (Figures 2, 5b and c). Such observations suggest that with an increase of particle size, the electrical mobility of unipolar diffusion charged particles becomes less accurate to the registered particle diameter (Morawska et al. 2009b).

Diesel soot #12 particles were generated at high total *PN* concentrations ($1.2 \pm 0.09 \times 10^5$ cm^{-3} reported by the UCPC). Total *PN* concentrations measured by NanoScan were statistically significantly higher (*p-value* < 0.05) than the reference by >20% ($1.9 \pm 0.2 \times 10^5$ cm^{-3}), whereas SMPS-L underestimated the reference concentration by $4 \pm 8\%$ (*p-value* > 0.05; not statistically significant) (Figure 1 and Table 3). The diesel soot #12 particle size distribution (Figure 6) measured with NanoScan was found to agree well with the internal reference SMPS-L (96 $\pm$ 0.5 nm) (Figure 2). The recent study of Stabile et al. (2014), observed similar results such as an up to twofold overestimation of the actual total particle number concentration obtained through the laboratory SMPS and pointed the effect of particle morphology on the NanoScan particle charging technique should be a possible explanation of the deviations on particle counting. The reason for the better agreement between the reference and measured particle diameters by NanoScan for diesel soot #12 with regard to spark generated soot at high concentrations #11 may be that freshly emitted diesel soot particles are often covered with volatile organic compounds, likely giving the particles a more compact shape than the spark-generated soot particles. The corresponding TEM image (Figure 6) revealed diesel soot particles as fairly compact agglomerates of smaller spherical particles of approximately 100 nm as physical diameter, which is

Figure 6. (Left) Measurement data and fitted particle number size distribution of generated 96 nm diesel soot particles at high concentrations, measured in the exposure chamber with SMPS-L and NanoScan. Error bars indicate the standard deviation. $p = p$-value. (Right) TEM image of collected diesel soot particles.

in a good agreement with the modal diameter reported by the SMPS-L and NanoScan.

Based on these findings, the NanoScan seems to be a useful instrument to estimate particle size distribution in occupational environments where the target particles are considered as agglomerated. However, total particle number concentrations can be overestimated by up to 66% (see previous sections). For accurate exposure assessment studies (e.g., in the tier 3 of a tiered exposure assessment strategy; Methner et al. 2010; Witschger et al. 2012; Asbach et al. 2014), the stationary SMPS instruments are still the preferred choice to measure simultaneously the total particle number concentration and size distribution.

3.2. Multimodal aerosols

Concerning the multimodal aerosols, the comparison between the NanoScan with the internal reference is shown in Table 4.

Bimodal diesel soot #13 (31 + 136 nm) and NaCl #14 (27 + 61 nm) and trimodal NaCl/DEHS #15 (27 + 54 + 145 nm), were generated at high total PN concentrations

$(2.3 \pm 0.07 \times 10^5$ cm^{-3}, $1.7 \pm 0.04 \times 10^5$ cm^{-3} and $2.9 \pm 0.4 \times 10^5$ cm^{-3} reported by UCPC, respectively). Total PN concentrations measured by NanoScan were below the reference by <20% for all the multimodal aerosols besides considered statistically significant (p-value < 0.05). The SMPS-L and SMPS-N overestimate the reference concentration by 50% and 47%, respectively, for the bimodal NaCl aerosol #14 (p-value < 0.05). Although better agreement from NanoScan with regard to total N concentrations, the corresponding fitted particle size distributions were found to not agree well with the internal reference SMPS-L and SMPS-N for the bimodal NaCl #14 (Figure S6 in the SI) and the trimodal NaCl/DEHS #15 (Figure S6 in the SI) since an unimodal distribution was obtained in both cases, delivering mode diameters of 51 ± 0.7 and 67 ± 1.1 nm, respectively, which correspond to the predominant mode size of the total particle number size distribution. Therefore, the NanoScan does not seem to be able to properly resolve multimodal distributions.

Only in case of bimodal diesel soot #13, the size distribution delivered by NanoScan may be interpreted as bimodal, however, its shape and modal diameters are

Table 4. Parameters of the fitted lognormal particle number size distributions (total number concentrations, modal diameter, and standard deviations) measured by the SMPSs (NanoScan, SMPS-L and SMPS-N) and UCPC measuring multimodal aerosols (number 13 to 15 in Table S1 in the SI); all concentrations (PN_total) in [cm^{-3}] and all diameters (D_mode) in [nm].

No. of experiment		Multimodal aerosols		
		Diesel soot #13	NaCl #14	NaCl/DEHS #15
UCPC $PN_{total} \pm \sigma$ [cm^{-3}]		**2.3 ± 0.07 × 10⁵**	**1.7 ± 0.04 × 10⁵**	**2.9 ± 0.4 × 10⁵**
NanoScan	$PN_\text{total} \pm \sigma$ [cm^{-3}]	2.8 ± 0.1 × 10⁵	1.9 ± 0.2 × 10⁵	3.3 ± 0.9 × 10⁵
SMPS-L		2.5 ± 0.1 × 10⁵	2.5 ± 0.07 × 10⁵	4.1 ± 0.7 × 10⁵
SMPS-N		2.7 ± 0.2 × 10⁵	2.5 ± 0.1 × 10⁵	3.2 ± 0.5 × 10⁵
NanoScan	$D_\text{mode} \pm \sigma$ [nm]	30.9 ± 1.9/48.1 ± 2.2	50.9 ± 0.7	66.6 ± 1.1
SMPS-L		**30.7 ± 0.1/136.4 ± 1.1**	**27.4 ± 0.2/61.0 ± 0.3**	**26.9 ± 0.5/53.8 ± 0.4/145.4 ± 2.6**
SMPS-N		31.1 ± 0.1/99.4 ± 2.3	27.0 ± 0.2/59.6 ± 0.3	23.2 ± 0.4/51.9 ± 0.3/116.5 ± 5.9

σ: Standard deviation.
Values in bold: considered internal reference value for total PN concentration (UCPC) and for particle number size distributions (SMPS-N or SMPS-L).
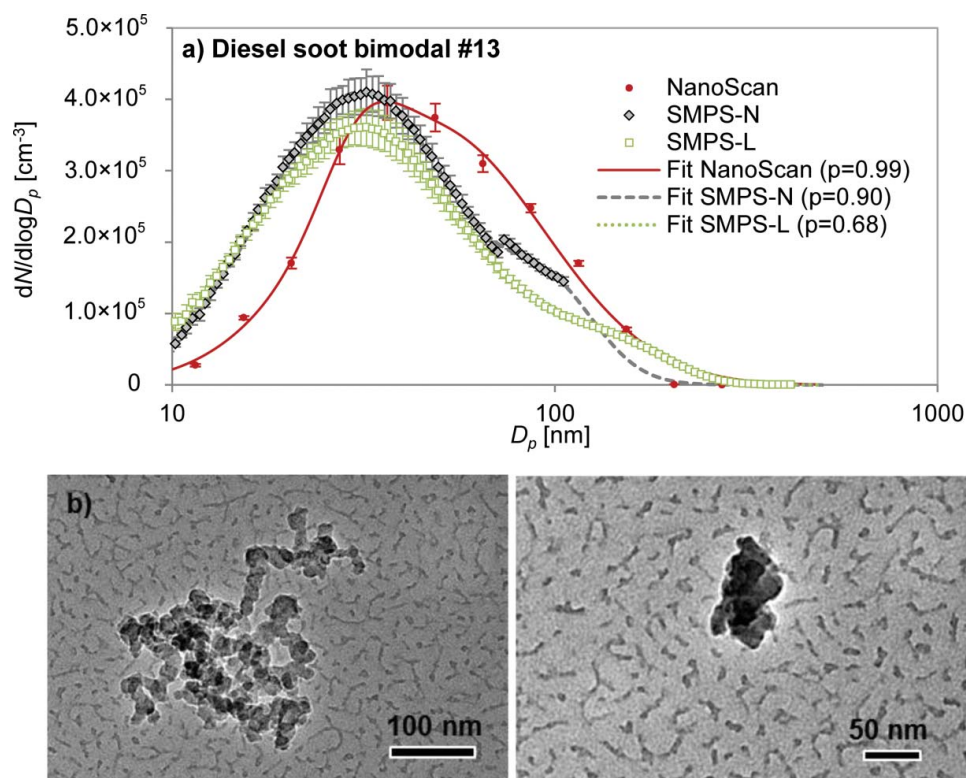
Figure 7. (a) Measurement data and fitted particle number size distribution of generated bimodal diesel soot, measured in the exposure chamber with SMPSs and NanoScan. Error bars indicate the standard deviation. $p = p$-value. (b) TEM images of collected 136 nm (left) and 31 nm (right) diesel soot particles.

very different from the ones measured with SMPS-L (Figure 7a). Generated diesel soot particles sampled on TEM grids are shown in Figure 7b. The TEM images revealed diesel soot particles as compact agglomerates of spherical primary particles, which fairly agrees with the modal diameters reported by the SMPS-L and the smaller diameter reported by NanoScan (31.1 ± 0.1 nm). Therefore, the NanoScan under-represented the actual diesel soot particle size of 136 nm delivering a mobility diameter much smaller maybe due to its open structure (seen in Figure 7b).

4. Conclusions

The present study compared the performance of the novel portable NanoScan SMPS TSI 3910 to two reference stationary SMPS instruments (one equipped with a nano-DMA, the other a long-DMA) an ultrafine condensation particle counter (UCPC). The instruments were challenged with five aerosol types with variable morphology and concentrations. The performance of the Nano-Scan was evaluated with regard to PN concentrations and size distributions and the main findings are summarised as follow:

4.1. Total particle number concentration

- NanoScan was able to measure compact and spherical particles (NaCl and DEHS) with a reasonable agreement with an UCPC in terms of *PN* concentration for particles between 60 nm and 230 nm in diameter, but showed significantly higher deviations for agglomerated particles especially when the spark soot agglomerates were larger and at high concentration (overestimation of 66% compared with the total particle number concentration obtained with the reference UCPC).

- *PN* concentrations measured by NanoScan tended to overestimate those reported by the UCPC, particularly for agglomerated particles such as ZnO, spark generated soot, and diesel soot particles (with relative differences >20%), likely because of the differences in the charging efficiency of the NanoScan unipolar charger for compact and agglomerated particles. These observations are consistent with Stabile et al. (2014) who conclude that the Nano-Scan is not able to properly measure diesel-generated particles (fresh aerosol made up of aggregated particles).

- The clear underestimation of 11 nm NaCl particles' *PN* concentration by the NanoScan evidences difficulties to accurately determine *PN* at the lower end of the instrument's particle size measurement range.
- Stationary SMPSs reproduced better agreements with UCPC with regard to *PN* than NanoScan when measuring agglomerated particles such as ZnO, spark soot and diesel soot particles (with relative differences <15% with respect to UCPC).

4.2. Particle size distributions

- Results from NanoScan were comparable to those measured by SMPSs (considering an arbitrary 20% threshold) with regard to particle diameter, for most of the aerosols measured, with the exception of 11 nm NaCl and DEHS particles.
- Particle size tended to be underestimated by Nano-Scan for spherical particles larger than 200 nm (by up to 34%).
- The NanoScan does not seem to be able to properly resolve multimodal distributions.

NanoScan results and their comparability with an SMPS show dependence on particle size, particle morphology, particle composition, and particle concentration. Different charge levels acquired by the particles in the unipolar charger might be the reason of this dependence. Although NanoScan instrument is known to provide higher time resolution analysis than the stationary SMPSs, it could be considered slow in certain specific microenvironments but it can be a useful instrument to obtain estimates of the size distribution in workplace air. Due to its portability, it is a valuable tool for simplified exposure assessment, e.g., in the second tier of a tiered exposure assessment strategy (Methner et al. 2010; Witschger et al. 2012; Asbach et al. 2014). However, its accuracy should not be overestimated. While the sizing accuracy was mostly within ±25%, measured total concentrations in some cases deviated by more than 50% (especially for agglomerated particles). For accurate measurements, e.g., in tier 3, stationary SMPS instruments are still the preferred choice.

Funding

References

Agarwal, J. K., Sem, G. J. (1980), Continuous flow, single-particle-counting condensation nucleus counter. *J.Aerosol Sci.*, 11(4):343–357. doi: http://dx.doi.org/10.1016/0021-8502(80)90042-7

Asbach, C., Fissan, H., Kaminski, H., Kuhlbusch, T. A. J., Pui, D. Y. H., Shin, H., Horn, H. G., Hase, T. (2011), A Low Pressure Drop Pre-Separator For Elimination of Particles Larger than 450 nm. *Aerosol &Air Qual. Res.*, 11:487–496.

Asbach, C., Kaminski, H., Fissan, H., Monz, C., Dahmann, D., Mülhopt, S., Paur, H., Kiesling, H., Herrmann, F., Voetz, M., Kuhlbusch, T. J. (2009), Comparison of Four Mobility Particle Sizers With Different Time Resolution for Stationary Exposure Measurements. *J. Nanopart. Res.*, 11(7):1593–1609. doi: 10.1007/s11051-009-9679-x

Asbach, C., Kaminski, H., von Barany, D., Kuhlbusch, T. A., Monz, C., Dziurowitz, N., Pelzer, J., Vossen, K., Berlin, K., Dietrich, S., Gotz, U., Kiesling, H. J., Schierl, R., Dahmann, D. (2012), Comparability of Portable Nanoparticle Exposure Monitors. *Ann. Occup. Hyg.*, 56(5):606–621.

Asbach, C., Kuhlbusch, T. A. J., Stahlmecke, B., Kaminski, H., Kiesling, H. J., Voetz, M., Dahmann, D., Götz, U., Dziurowitz, N., Plitzko, S. (2014). *Measurement and Monitoring Strategy for Assessing Workplace Exposure to Airborne Nanomaterials*. Taylor & Francis, Abingdon, UK.

Asmi, A., Wiedensohler, A., Laj, P., Fjaeraa, A. M., Sellegri, K., Birmili, W., Weingartner, E., Baltensperger, U., Zdimal, V., Zikova, N., Putaud, J. P., Marinoni, A., Tunved, P., Hansson, H. C., Fiebig, M., Kivekäs, N., Lihavainen, H., Asmi, E., Ulevicius, V., Aalto, P.P., Swietlicki, E., Kristensson, A., Mihalopoulos, N., Kalivitis, N., Kalapov, I., Kiss, G., de Leeuw, G., Henzing, B., Harrison, R. M., Beddows, D., O'Dowd, C., Jennings, S. G., Flentje, H., Weinhold, K., Meinhardt, F., Ries, L., Kulmala, M. (2011), Number Size Distributions and Seasonality Of Submicron Particles in Europe 2008–2009. *Atmos. Chem. Phys.*, 11(11):5505–5538. doi: 10.5194/acp-11-5505-2011

Atkinson, R. W., Anderson, H. R., Sunyer, J., Ayres, J., Baccini, M., Vonk, J. M., Boumghar, A., Forastiere, F., Forsberg, B., Touloumi, G., Schwartz, J., Katsouyanni, K. (2001), Acute effects of Particulate Air Pollution on Respiratory Admissions: Results From APHEA 2 Project. Air Pollution and Health: A European Approach. [Research Support, Non-U S Gov't]. *Am. J. Respir. Crit. Care Med.*, 164(10 Pt 1):1860–1866.

Beddows, D. C. S., Dall'Osto, M., Harrison, R. M., Kulmala, M., Asmi, A., Wiedensohler, A., Laj, P., Fjaeraa, A. M., Sellegri, K., Birmili, W., Bukowiecki, N., Weingartner, E., Baltensperger, U., Zdimal, V., Zikova, N., Putaud, J. P., Marinoni, A., Tunved, P., Hansson, H. C., Fiebig, M., Kivekäs, N., Swietlicki, E., Lihavainen, H., Asmi, E., Ulevicius, V., Aalto, P. P., Mihalopoulos, N., Kalivitis, N., Kalapov, I., Kiss, G., de Leeuw, G., Henzing, B., O'Dowd, C., Jennings, S. G., Flentje, H., Meinhardt, F., Ries, L., Denier van der Gon, H. A. C., Visschedijk, A. J. H. (2014) Variations in Tropospheric Submicron Particle Size Distributions Across the

European Continent 2008–2009. *Atmos. Chem. Phys.*, 14 (8):4327–4348. doi: 10.5194/acp-14-4327-2014

Biskos, G., Mastorakos, E., Collings, N. (2004), Monte-Carlo Simulation of Unipolar Diffusion Charging for Spherical And Non-Spherical Particles. *J.Aerosol Sci.*, 35(6):707–730. doi: http://dx.doi.org/10.1016/j.jaerosci.2003.11.010

Brines, M., Dall'Osto, M., Beddows, D. C. S., Harrison, R. M., Gómez-Moreno, F., Núñez, L., Artíñano, B., Costabile, F., Gobbi, G. P., Salimi, F., Morawska, L., Sioutas, C., Querol, X. (2015), Traffic and Nucleation Events as Main Sources Of Ultrafine Particles In High-Insolation Developed World Cities. *Atmos. Chem. Phys.*, 15(10):5929–5945. doi: 10.5194/acp-15-5929-2015

Brouwer, D. (2010), Exposure to Manufactured Nanoparticles in Different Workplaces. *Toxicol.*, 269(2–3):120–127.

Buonanno, G., Morawska, L., Stabile, L., Viola, A. (2010), Exposure to Particle Number, Surface Area and PM Concentrations In Pizzerias. *Atmos. Environ.*, 44(32):3963–3969. doi: http://dx.doi.org/10.1016/j.atmosenv.2010.07.002

Buonanno, G., Stabile, L., Morawska, L., Russi, A. (2013), Children Exposure Assessment to Ultrafine Particles and Black Carbon: The Role of Transport and Cooking Activities. *Atmos. Environ.*, 79(0):53–58. doi: http://dx.doi.org/10.1016/j.atmosenv.2013.06.041

Chen, D. R., Pui, D. Y. H., Hummes, D., Fissan, H., Quant, F. R., Sem, G. J. (1998), Design and Evaluation of a Nanometer Aerosol Differential Mobility Analyzer (Nano-DMA). *J. Aerosol Sci.*, 29(5–6):497–509. doi: http://dx.doi.org/10.1016/S0021-8502(97)10018-0

Costabile, F., Birmili, W., Klose, S., Tuch, T., Wehner, B., Wiedensohler, A., Franck, U., König, K., Sonntag, A. (2009), Spatio-Temporal Variability and Principal Components of the Particle Number Size Distribution in an Urban Atmosphere. *Atmos. Chem. Phys.*, 9(9):3163–3195. doi: 10.5194/acp-9-3163-2009

Cusack, M., Pérez, N., Pey, J., Wiedensohler, A., Alastuey, A., Querol, X. (2013). Variability of Sub-micrometer Particle Number Size Distributions and Concentrations in the Western Mediterranean Regional Background. *Tellus B*, 65:1–19.

Demou, E., Peter, P., Hellweg, S. (2008) Exposure to Manufactured Nanostructured Particles in an Industrial Pilot Plant. *Ann. Occup. Hyg.*, 52(8):695–706. doi: 10.1093/annhyg/men058

Dixkens, J., Fissan, H. (1999), Development of an Electrostatic Precipitator for Off-Line Particle Analysis. *Aerosol Sci. Technol.*, 30(5):438–453. doi: 10.1080/027868299304480

Dockery, D. W., Pope, C. A., 3rd, Xu, X., Spengler, J. D., Ware, J. H., Fay, M. E., Ferris, B. G., Jr., Speizer, F. E. (1993), An association Between Air Pollution and Mortality in Six U.S. Cities. *N. Engl. J. Med.*, 329(24):1753–1759.

Donaldson, K., Aitken, R., Tran, L., Stone, V., Duffin, R., Forrest, G., Alexander, A. (2006), Carbon Nanotubes: A Review of Their Properties in Relation to Pulmonary Toxicology and Workplace Safety. *Toxicol. Sci.*, 92(1):5–22. doi: 10.1093/toxsci/kfj130

Fissan, H., Helsper, C., Thielen, H. J. (1983), Determination of Particle Size Distribution by Means of an Electrostatic Classifier. *J. Aerosol Sci.*, 14:354–357.

Fissan, H., Hummes, D., Stratmann, F., Büscher, P., Neumann, S., Pui, D. Y. H., Chen, D. (1996), Experimental Comparison of Four Differential Mobility Analyzers for Nanometer Aerosol Measurements. *Aerosol Sci. Technol.*, 24(1):1–13. doi: 10.1080/02786829608965347

Fissan, H., Pöcher, A., Neumann, S., Boulaud, D., Pourprix, M. (1998), Analytical and Empirical Transfer Functions of a simplified spectromètre de mobilité electrique circulaire (SMEC) for Nano Particles. *J. Aerosol Sci.*, 29(3):289–293. doi: http://dx.doi.org/10.1016/S0021-8502(97)10014-3

Fonseca, A. S., Viana, M., Querol, X., Moreno, N., de Francisco, I., Estepa, C., de la Fuente, G. F. (2015a), Ultrafine and Nanoparticle Formation and Emission Mechanisms During Laser Processing of Ceramic Materials. *J.Aerosol Sci.*, 88:48–57. doi: http://dx.doi.org/10.1016/j.jaerosci.2015.05.013

Fonseca, A. S., Viitanen, A. K., Koivisto, A. J., Kangas, A., Huhtiniemi, M., Hussein, T., Vanhala, E., Viana, M., Querol, X., Hameri, K. (2015b). Characterization of Exposure to Carbon Nanotubes in an Industrial Setting. *Ann. Occup. Hyg.*, 59(5):586–599.

Fuchs, N. A. (1963), On the Stationary Charge Distribution on Aerosol Particles in a Bipolar Ionic Atmosphere. *Geofisica Pura e Applicata*, 56(1):185–193. doi: 10.1007/bf01993343

Gómez-Moreno, F. J., Alonso, E., Artíñano, B., Juncal-Bello, V., Iglesias-Samitier, S., Piñeiro Iglesias, M., Mahía, P. L., Pérez, N., Pey, J., Ripoll, A., Alastuey, A., de la Morena, B. A., García, M. I., Rodríguez, S., Sorribas, M., Titos, G., Lyamani, H., Alados-Arboledas, L., Latorre, E., Tritscher, T., Bischof, O. F. (2015), Intercomparisons of Mobility Size Spectrometers and Condensation Particle Counters in the Frame of the Spanish Atmospheric Observational Aerosol Network. *Aerosol Sci. Technol.*, 49(9):777–785. doi: 10.1080/02786826.2015.1074656

Hering, S. V., Stolzenburg, M.R., Quant, F. R., Oberreit, D. R., Keady, P. B. (2005). A Laminar-Flow, Water-Based Condensation Particle Counter (WCPC). *Aerosol Sci. Technol.*, 39(7):659–672. doi: 10.1080/02786820500182123

Hermann, M., Wehner, B., Bischof, O., Han, H. S., Krinke, T., Liu, W., Zerrath, A., Wiedensohler, A. (2007), Particle Counting Efficiencies of New TSI Condensation Particle Counters. *J Aerosol Sci.*, 38(6):674–682. doi: http://dx.doi.org/10.1016/j.jaerosci.2007.05.001

Hoppel, W. A. (1978), Determination of the Aerosol Size Distribution From the Mobility Distribution of the Charged Fraction of Aerosols. *J.Aerosol Sci.*, 9(1):41–54. doi: http://dx.doi.org/10.1016/0021-8502(78)90062-9

Jeong, C.-H., Evans, G. J. (2009), Inter-Comparison of a Fast Mobility Particle Sizer and a Scanning Mobility Particle Sizer Incorporating an Ultrafine Water-Based Condensation Particle Counter. *Aerosol Sci.Technol.*, 43(4):364–373. doi: 10.1080/02786820802662939

Jung, H., Kittelson, D. B. (2005), Characterization of Aerosol Surface Instruments in Transition Regime. *Aerosol Sci. Technol.*, 39(9):902–911. doi: 10.1080/02786820500295701

Kaminski, H., Kuhlbusch, T. A. J., Rath, S., Götz, U., Sprenger, M., Wels, D., Polloczek, J., Bachmann, V., Dziurowitz, N., Kiesling, H.-J., Schwiegelshohn, A., Monz, C., Dahmann, D., Asbach, C. (2013), Comparability of Mobility Particle Sizers and Diffusion Chargers. *J. Aerosol Sci.*, 57(0):156–178. doi: http://dx.doi.org/10.1016/j.jaerosci.2012.10.008

Knutson, E. O., Whitby, K. T. (1975), Aerosol Classification by Electric Mobility: Apparatus, Theory, and Applications. *J. Aerosol Sci.*, 6(6):443–451. doi: http://dx.doi.org/10.1016/0021-8502(75)90060-9

Koivisto, A. J., Lyyranen, J., Auvinen, A., Vanhala, E., Hameri, K., Tuomi, T., Jokiniemi, J. (2012), Industrial Worker Exposure to Airborne Particles During the Packing of Pigment and Nanoscale Titanium Dioxide. *Inhal Toxicol.*, 24(12):839–849.

Koivisto, A. J., Palomaki, J. E., Viitanen, A. K., Siivola, K. M., Koponen, I. K., Yu, M., Kanerva, T. S., Norppa, H., Alenius, H. T., Hussein, T., Savolainen, K. M., Hameri, K. J. (2014), Range-finding Risk Assessment of Inhalation Exposure to Nanodiamonds in a Laboratory Environment. [Research Support, Non-U S Gov't]. *Int. J. Environ. Res. Public Health*, 11(5):5382–5402.

Kousaka, Y., Okuyama, K., Adachi, M. (1985), Determination of Particle Size Distribution of Ultra-Fine Aerosols Using a Differential Mobility Analyzer. *Aerosol Sci. Technol.*, 4 (2):209–225. doi: 10.1080/02786828508959049

Kreyling, W. G., Semmler, M., Erbe, F., Mayer, P., Takenaka, S., Schulz, H., Oberdorster, G., Ziesenis, A. (2002), Translocation of Ultrafine Insoluble Iridium Particles from Lung Epithelium to Extrapulmonary Organs is Size Dependent but very Low. *J. Toxicol. Environ. Health A.*, 65(20):1513–1530.

Kuhlbusch, T., Asbach, C., Fissan, H., Gohler, D., Stintz, M. (2011), Nanoparticle Exposure at Nanotechnology Workplaces: A Review. *Partic. Fibre Toxicol.*, 8(1):22.

Leskinen, J., Joutsensaari, J., Lyyränen, J., Koivisto, J., Ruusunen, J., Järvelä, M., Tuomi, T., Hämeri, K., Auvinen, A., Jokiniemi, J. (2012), Comparison of Nanoparticle Measurement Instruments for Occupational Health Applications. *J. Nanopart. Res.*, 14(2):1–16. doi: 10.1007/s11051-012-0718-7

Levin, M., Gudmundsson, A., Pagels, J. H., Fierz, M., Mølhave, K., Löndahl, J., Jensen, K. A., Koponen, I. K. (2015), Limitations in the use of Unipolar Charging for Electrical Mobility Sizing Instruments: A Study of the Fast Mobility Particle Sizer. *Aerosol Sci. Technol.*, 49(8):556–565. doi: 10.1080/02786826.2015.1052039

Liu, B. Y. H., Pui, D. Y. H. (1974), A Submicron Aerosol Standard and the Primary, Absolute Calibration of the Condensation Nuclei counter. *J. Colloid Interf. Sci.*, 47(1):155–171. doi: http://dx.doi.org/10.1016/0021-9797(74)90090-3

Maynard, A., Kuempel, E. (2005), Airborne Nanostructured Particles and Occupational Health. *J. Nanopart. Res.*, 7 (6):587–614. doi: 10.1007/s11051-005-6770-9

Medved, A., Dorman, F., Kaufman, S. L., Pöcher, A. (2000), A New Corona-based Charger for Aerosol Particles. *J. Aerosol. Sci.*, 31:S616–S661.

Methner, M., Hodson, L., Geraci, C. (2010), Nanoparticle Emission Assessment Technique (NEAT) for the Identification and Measurement of Potential Inhalation Exposure to Engineered Nanomaterials–part A. *J. Occup. Environ. Hyg.*, 7(3):127–132.

Monsé, C., Monz, C., Dahmann, D., Asbach, C., Stahlmecke, B., Lichtenstein, N., Buchwald, K.-E., Merget, R., Bünger, J., Brüning, T. (2014), Development and Evaluation of a Nanoparticle Generator for Human Inhalation Studies with Airborne Zinc Oxide. *Aerosol Sci. Technol.*, 48(4):418–426. doi: 10.1080/02786826.2014.883064

Morawska, L., He, C., Johnson, G., Guo, H., Uhde, E., Ayoko, G. (2009a). Ultrafine Particles in Indoor Air of a School: Possible Role of Secondary Organic Aerosols. *Environ. Sci. & Technol.*, 43(24):9103–9109. doi: 10.1021/es902471a

Morawska, L., Wang, H., Ristovski, Z., Jayaratne, E. R., Johnson, G., Cheung, H. C., Ling, X., He, C. (2009b), JEM Spotlight: Environmental Monitoring of Airborne Nanoparticles. [Review]. *J. Environ. Monit.*, 11(10):1758–1773.

Oberdörster, G., Oberdorster, E., Oberdorster, J. (2005), Nanotoxicology: An Emerging Discipline Evolving from Studies of Ultrafine Particles. *Environ. Health Perspect.*, 113 (7):823–839.

Oberdörster, G., Sharp, Z., Atudorei, V., Elder, A., Gelein, R., Kreyling, W., Cox, C. (2004), Translocation of Inhaled Ultrafine Particles to the Brain. *Inhal. Toxicol.*, 16(6-7):437–445.

Peters, A., Wichmann, H. E., Tuch, T., Heinrich, J., Heyder, J. (1997), Respiratory Effects are Associated with the Number of Ultrafine Particles. *Am. j. resp. crit. care med..*, 155 (4):1376–1383. doi: 10.1164/ajrccm.155.4.9105082

Price, H. D., Stahlmecke, B., Arthur, R., Kaminski, H., Lindermann, J., Däuber, E., Asbach, C., Kuhlbusch, T. A. J., BéruBé, K. A., Jones, T. P. (2014), Comparison of Instruments for Particle Number Size Distribution Measurements in Air Quality Monitoring. *J. Aerosol Sci.*, 76(0):48–55. doi: http://dx.doi.org/10.1016/j.jaerosci.2014.05.001

Qi, C., Asbach, C., Shin, W. G., Fissan, H., Pui, D. Y. H. (2009), The Effect of Particle Pre-Existing Charge on Unipolar Charging and Its Implication on Electrical Aerosol Measurements. *Aerosol Sci. Technol.*, 43(3):232–240. doi: 10.1080/02786820802587912

Reche, C., Querol, X., Alastuey, A., Viana, M., Pey, J., Moreno, T., Rodríguez, S., González, Y., Fernández-Camacho, R., de la Rosa, J., Dall'Osto, M., Prévôt, A. S. H., Hueglin, C., Harrison, R. M., Quincey, P. (2011), New Considerations for PM, Black Carbon and Particle Number Concentration for Air Quality Monitoring Across Different European Cities. *Atmos. Chem. Phys.*, 11(13):6207–6227. doi: 10.5194/acp-11-6207-2011

Reineking A, Porstendörfer J (1986). Measurement of Particle Loss Functions in a Differential Mobility Analyzer (TSI, Model 3071) for Different Flow Rates. *Aerosol Sci. Technol.*, 27:483–486

Stabile, L., Cauda, E., Marini, S., Buonanno, G. (2014), Metrological Assessment of a Portable Analyzer for Monitoring the Particle Size Distribution of Ultrafine Particles. *Ann. Occup. Hyg.*, 58(7):860–876. doi: 10.1093/annhyg/meu025

Tammet, H., Mirme, A., Tamm, E. (2002), Electrical Aerosol Spectrometer of Tartu University. *Atmos. Res.*, 62(3–4):315–324. doi: http://dx.doi.org/10.1016/S0169-8095(02)00017-0

ten Brink, H. M., Plomp, A., Spoelstra, H., van de Vate, J. F. (1983), A High-Resolution Electrical Mobility Aerosol Spectrometer (MAS). *J. Aerosol Sci.*, 14(5):589–597. doi: http://dx.doi.org/10.1016/0021-8502(83)90064-2

Tritscher, T., Beeston, M., Zerrath, A.F., Elzey, S., Krinke, T. J., Filimundi, E., Bischof, O. F. (2013), NanoScan SMPS–A Novel, Portable Nanoparticle Sizing and Counting Instrument. *J. Phy. Conf. Ser.*, 429(1):012061.

TSI. (2015), Choosing the right CPC for your application. APPLICATION NOTE CPC-002 (US). APPLICATION NOTE CPC-002 (US), from http://www.tsi.com/uploaded Files/_Site_Root/Products/Literature/Application_Notes/CPC-002-appnote.pdf

Voliotis, A., Bezantakos, S., Giamarelou, M., Valenti, M., Kumar, P., Biskos, G. (2014), Nanoparticle Emissions from Traditional Pottery Manufacturing. [Research Support, Non-U S Gov't]. Environ. Sci. Process Impacts, 16(6):1489–1494.

Wang, S. C., Flagan, R. C. (1989), Scanning Electrical Mobility Spectrometer. *J. Aerosol Sci.*, 20(8):1485–1488. doi: http://dx.doi.org/10.1016/0021-8502(89)90868-9

Wang, S. C., Flagan, R. C. (1990), Scanning Electrical Mobility Spectrometer. *Aerosol Sci.Tech.*, 13(2):230–240. doi: 10.1080/02786829008959441

Watson, J. G., Chow, J. C., Sodeman, D. A., Lowenthal, D. H., Chang, M. C. O., Park, K., Wang, X. (2011,. Comparison of Four Scanning Mobility Particle Sizers at the Fresno Supersite. *Particuology*, 9(3):204–209. doi: http://dx.doi.org/10.1016/j.partic.2011.03.002

Wehner, B., Birmili, W., Gnauk, T., Wiedensohler, A. (2002), Particle Number Size Distributions in a Street Canyon and their Transformation into the Urban-Air Background: Measurements and a Simple Model Study. *Atmos. Environ.*, 36(13):2215–2223. doi: http://dx.doi.org/10.1016/S1352-2310(02)00174-7

Wiedensohler, A., Birmili, W., Nowak, A., Sonntag, A., Weinhold, K., Merkel, M., Wehner, B., Tuch, T., Pfeifer, S., Fiebig, M., Fjäraa, A. M., Asmi, E., Sellegri, K., Depuy, R., Venzac, H., Villani, P., Laj, P., Aalto, P., Ogren, J. A., Swietlicki, E., Williams, P., Roldin, P., Quincey, P., Hüglin, C., Fierz-Schmidhauser, R., Gysel, M., Weingartner, E., Riccobono, F., Santos, S., Grüning, C., Faloon, K., Beddows, D., Harrison, R., Monahan, C., Jennings, S. G., O'Dowd, C. D., Marinoni, A., Horn, H. G., Keck, L., Jiang, J., Scheckman, J., McMurry, P. H., Deng, Z., Zhao, C. S., Moerman, M., Henzing, B., de Leeuw, G., Löschau, G., Bastian, S. (2012), Mobility Particle Size Spectrometers: Harmonization of Technical Standards and Data Structure to Facilitate High Quality Long-Term Observations of Atmospheric Particle Number Size Distributions. *Atmos. Meas. Tech.*, 5(3):657–685. doi: 10.5194/amt-5-657-2012

Wiedensohler, A., Orsini, D., Covert, D. S., Coffmann, D., Cantrell, W., Havlicek, M., Brechtel, F. J., Russell, L. M., Weber, R. J., Gras, J., Hudson, J. G., Litchy, M. (1997), Intercomparison Study of the Size-Dependent Counting Efficiency of 26 Condensation Particle Counters. *Aerosol Sci.Tech.*, 27(2):224–242. doi: 10.1080/02786829708965469

Winklmayr, W., Reischl, G. P., Lindner, A. O., Berner, A. (1991), A New Electromobility Spectrometer for the Measurement of Aerosol Size Distributions in the Size Range from 1 to 1000 nm. *J Aerosol Sci.*, 22(3):289–296. doi: http://dx.doi.org/10.1016/S0021-8502(05)80007-2

Witschger, O., Bihan, O., Reynier, M., Durand, C., Marchetto, A., Zimmermann, E., Charpentier, D. (2012), Préconisation en matière de caractérisation et d'exposition des potentiels d'emission et d'exposition professionnelle aux aerosols lors d'operations nanomateriaux. INRS- Hygiène et sécurité du travail ND 2355-226-12, 41-55.

Zhang, Q., Gangupomu, R. H., Ramirez, D., Zhu, Y. (2010), Measurement of Ultrafine Particles and other Air Pollutants Emitted by Cooking Activities. [Research Support, U S Gov't, Non-P H S]. *Int. J. Environ. Res. Public Health*, 7 (4):1744–1759.

Zhang, S.-H., Akutsu, Y., Russell, L. M., Flagan, R.C., Seinfeld, J. H. (1995), Radial Differential Mobility Analyzer. *Aerosol Sci Tech.*, 23(3):357–372. doi: 10.1080/02786829508965320

Zimmerman, N., Godri Pollitt, K. J., Jeong, C.-H., Wang, J. M., Jung, T., Cooper, J.M., Wallace, J.S., Evans, G.J. (2014), Comparison of Three Nanoparticle Sizing Instruments: The Influence of Particle Morphology. *Atmos. Environ.*, 86:140–147. doi: http://dx.doi.org/10.1016/j.atmosenv.2013.12.023

Zimmerman, N., Jeong, C.-H., Wang, J. M., Ramos, M., Wallace, J. S., Evans, G. J. (2015), A Source-independent Empirical Correction Procedure for the Fast Mobility and Engine Exhaust Particle Sizers. *Atmo. Environ.*, 100:178–184. doi: http://dx.doi.org/10.1016/j.atmosenv.2014.10.054